Thoracic Aortic Parallel Stent-Graft Behaviour When Subjected to Radial Loading

Jakub Kwiecinski[a,*], Christopher P. Cheng[b], Raman Uberoi[c], Mohammed Hadi[c], Philipp Hempel[d], Christoph Degel[d], Zhong You[a]

[a] *Department of Engineering Science, University of Oxford, Oxford, UK*
[b] *Division of Vascular Surgery, Stanford University, Stanford, CA, USA*
[c] *Department of Vascular Surgery, Oxford University Hospitals NHS Trust, Oxford, UK*
[d] *Admedes GmbH, Pforzheim, Germany*

Abstract

To manage complex aortic arch disease using minimally invasive techniques, interventionalists have reported the use of multiple stent-graft devices deployed in a parallel configuration. The structural device-device and device-artery interactions arising during aortic arch parallel endografting, also known as chimney thoracic endovascular aortic repair (ch-TEVAR), is not well understood. Through the use of a radial force testing system we sought to characterise both the loading and deformation behaviour of parallel endografts in representative ch-TEVAR configurations. Four commercially available devices (Bentley BeGraft, Gore TAG, Gore Viabahn, and Medtronic Valiant) were subjected to uniform radial load individually, and in six combinations, to quantify loading profiles. Image data collected during testing were analysed to evaluate mechanical deformations in terms of gutters, chimney and main endograft compression, as well as graft infolding. Parallel endografting was found to increase radial loads when compared to standard TEVAR. Chronic outward force during ch-TEVAR was dependent on main endograft manufacturer, with TAG combinations leading to consistently higher loads than Valiant, but independent of chimney graft type. Endograft deformations were dependent on chimney graft type, with Viabahn combinations presenting with lower gutter areas and increased lumen compression than BeGraft. Chimney graft deformations were also influenced by deployment arrangement in the case of double ch-TEVAR. This study emphasizes the significant variability in both radial loads and mechanical deformations between clinically relevant ch-TEVAR configurations.

Keywords: Stent-graft, Chimney graft, Parallel graft, Endograft, Gutter, Endoleak, Radial force, Thoracic Aortic Aneurysm, Dissection, Endovascular repair, TEVAR, Nitinol, Stent testing

1. Introduction

To ensure a complete aortic seal and to minimize risk of device migration during minimally invasive endovascular repair, stent-grafts should be sufficiently oversized. This oversizing (OS), however, results in radial loads exerted onto the aortic wall. As a consequence of these additional loads, recent studies have reported on microstructural changes to the aortic wall architecture [1] as well as aortic diameter enlargement [2], potentially compromising long-term treatment efficacy.

In an effort to assist interventional radiologists and surgeons, endograft manufacturers prescribe recommended device sizes corresponding to patient anatomy. These recommendations, however, are strictly limited to so-called "on-label" device use: patient, anatomy, and disease state profiles with demonstrated clinical evidence. In the case of complex endovascular procedures, whereby devices are often used in an "off-label" fashion (i.e. outside of their prescribed indication), no such guidance exists.

*Corresponding author: Jakub Kwiecinski (jkwiecin@gmail.com)

Indeed, management of aortic arch disease presents as one of the most technically challenging subsets of endovascular repair. To treat select patients, radiologists have augmented traditional endografting techniques using standard devices in an off-label manner. Known as chimney thoracic endovascular aortic repair (ch-TEVAR), this procedure employs multiple off-the-shelf devices deployed in a parallel configuration: a main endograft (MG) to exclude the diseased aorta from arterial blood flow, and peripheral chimney grafts (CGs) to maintain supra-aortic branch perfusion [3].

Although the technical feasibility and mid-term outcomes of ch-TEVAR have established its utility, this technique still suffers from high-risk complications [4]. Specifically, the formation of so-called "gutters", gaps which form between the endografts and aortic wall leading to type 1a endoleak, can render the treatment ineffective. To minimize the risk of gutter formation, radiologists often resort to deploying excessively oversized main endografts; it is thought that the additional main endograft circumference will better conform to both the aortic wall and chimney graft(s), enhancing the aortic seal.

Currently, there exists no consensus as to the optimal device combination or sizing strategy when performing such complex procedures in the aortic arch [5]. A series of reports have presented various methodologies for main endograft sizing in the case of ch-EVAR (treatment of abdominal aortic aneurysm, AAA), and have been proposed using an analytical approach [6–8]. Recently, Fazzini et al. [9] have described patient-specific ch-TEVAR sizing techniques and reported its use in a small case series of eight patients. Critically, these methods do not consider the potential impact of main endograft oversizing nor device type on the resulting radial loads exerted onto the aortic wall.

As such, the aim of this investigation was to: (1) characterise the radial loading behaviour of constituent ch-TEVAR devices individually, (2) determine the radial loading behaviour of parallel endografts representative of typical ch-TEVAR configurations, and (3) quantify the corresponding mechanical deformations of parallel endografts resulting from radial loading in a benchtop setup. It was hypothesised that both device type and configuration would influence ch-TEVAR interactions.

2. Materials and methods

2.1. Endografts

In this study, four commercially available endografts commonly used in ch-TEVAR were investigated. The main endografts included a self-expandable (SE) Conformable TAG Thoracic Endoprosthesis (W.L. Gore & Associates Inc., Flagstaff, AZ, USA) and a SE Valiant Thoracic Stent-Graft (Medtronic Inc., Santa Rosa, CA, USA). The chimney grafts included a SE Viabahn (W.L. Gore & Associates Inc., Flagstaff, AZ, USA) and a balloon-expandable (BE) BeGraft (Bentley Innomed GmbH, Hechingen, Germany). Deployed devices are shown in Figure 1 with specifications given in Table 1.

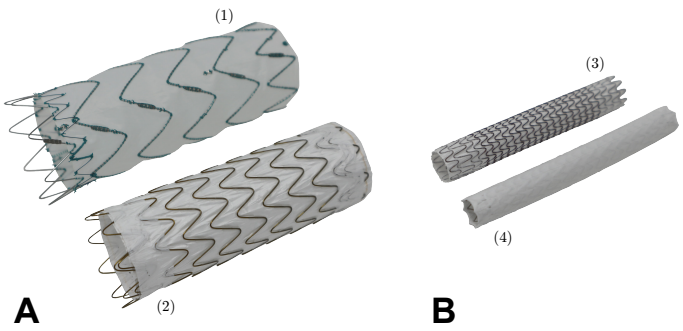

Figure 1: Endovascular devices considered in ch-TEVAR investigations. (A) Main endograft devices, including Medtronic Valiant (*1*) and Gore TAG (*2*); (B) chimney graft devices, including Gore Viabahn (*3*), and Bentley BeGraft (*4*). *Note:* devices shown are not to scale.

Table 1: Specifications and characteristics of the four endovascular devices investigated.

Device Feature	Main Endograft		Chimney Graft	
	TAG	Valiant	Viabahn	BeGraft
Labelled diameter (mm)	34.0	40.0	8.0	7.0
Measured length (mm)	105.0	117.0	50.0	55.0
IFU vessel dia. (mm)	27 - 32	35, 36	6.6 - 7.5	7.0
Degree OS range (%)	6.3 - 25.9	11.1, 14.3	6.7 - 21.2	n/a
Delivery diameter (Fr)	22	24	8	6
Stent material	Nitinol	Nitinol	Nitinol	CoCr
Graft material	ePTFE/FEP	PET	ePTFE/FEP	ePTFE
Deployment type	SE	SE	SE	BE
Stent frame type	Helical	Rings	Helical	Open Cell

IFU - instructions for use; *OS* - oversizing; 1 Fr = 1/3mm; *CoCr* - cobalt-chromium; *ePTFE* - expanded polytetrafluoroethylene; *FEP* - fluorinated ethylene propylene; *PET* - polyethylene terephthalate; *SE* - self-expandable; *BE* - balloon-expandable

2.2. Device characterisation

Each device was individually characterised by means of a conventional radial force test [10] synonymous to crimping (loading) and deployment (unloading) of self-expanding stents. In this mechanical loading regime, a uniform load is directed perpendicular to the longitudinal axis of a cylinder and applied to the outer cylindrical surface of the device. All testing was performed using an MSI RX650 Radial Expansion Force System (Machine Solutions Inc., Flagstaff, AZ, USA). The test system consists of a twelve-plate segmental compression mechanism, driven by a linear actuator, which is used to control the diameter of the testing aperture. An integrated load cell and encoder register the resulting diameter-load data.

Devices were deployed and subsequently placed into the testing system. SE stents were subjected to a single load-unload cycle, whereas the BeGraft was subjected to a stepped multi-cycle test. All experiments were run in displacement control at a rate of 0.1mm/s in a temperature-controlled heating chamber set at 37±2°C. The complete test setup is shown in Figure 2. Similar experimental systems and protocols have been described elsewhere to assess the radial loading behaviour of transcatheter aortic valves as well as venous stents [11–13].

Characterisation was based upon analysis of the resulting radial load profiles normalized by measured device length. For SE devices, the chronic outward force (COF) and the radial resistive force (RRF) [14] were quantified. The COF is the continual opening force of the SE device acting on the vessel wall at a specified diameter, as measured from the unloading portion of the radial load profile (i.e. during expansion). The RRF is the associated force generated by the SE device to resist compression, as measured from the loading portion of the radial load profile (i.e. during crimping). BE devices do not possess a COF or RRF per se, and thus BE stent radial strength is reported herein. To determine radial strength, the steepest portion of a substantially linear unloading curve is offset in a parallel manner so that its diametric intercept is at a specific diameter of interest. The intersection of the offset unloading line with the radial load profile establishes the device radial strength for a specified radial compression (which would have resulted in the plastic deformation of interest) [10]. For the sake of comparison, the BE unloading line was offset to the diameter equivalent to the maximum device oversizing of its SE counterpart.

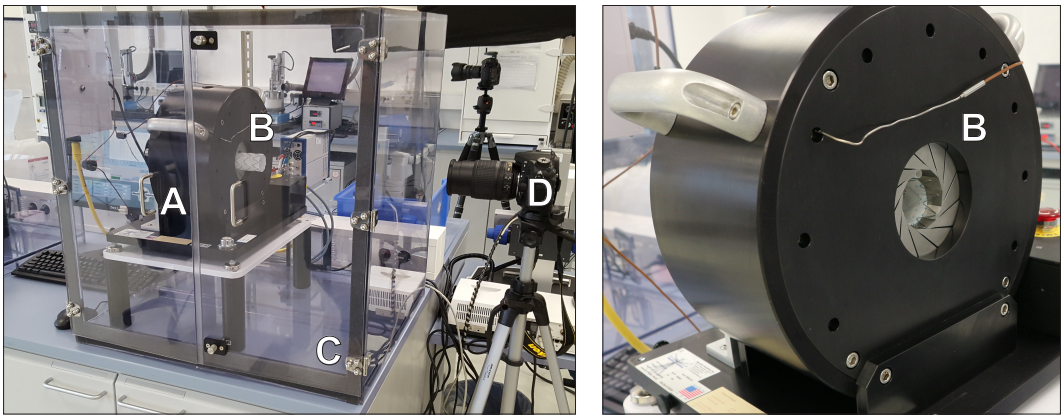

Figure 2: Benchtop radial loading test setup. (A) MSI RX650 radial force testing system measurement head; (B) twelve plate segmental compression mechanism; (C) enclosed heating chamber maintained at physiological temperature; (D) video acquisition aligned to the level of the compression mechanism aperture. *Note*: Valiant endograft partially inserted into compression mechanism at (*B, left*) for illustrative purposes only.

2.3. Radial loading during ch-TEVAR

To assess radial loads during ch-TEVAR, four single chimney combinations (TAG and Valiant MGs with either Viabahn or BeGraft CGs) and two double chimney combinations (TAG-Viabahn 2x and Valiant-Viabahn 2x) were subjected to radial loading-unloading in a manner similar to that described above. Specific details are provided below.

For ch-TEVAR combinations containing SE chimney grafts, the initial test aperture diameter was set 1mm less than the combined MG-CG diameter (i.e. radial loading initiated under a slightly compressed condition to ensure device-device interaction stability). Devices were positioned such that the chimney graft(s) extended 1-2mm proximal to the main endograft covering, and chimneys were aligned to lie between proximal main endograft stent struts where possible. In the case of double ch-TEVAR, chimney grafts were aligned in an adjacent fashion. Devices were radially loaded to a diameter equivalent to 60% main endograft oversizing, followed by unloading. A representative schematic of a SE single chimney initial configuration is given in Figure 3.

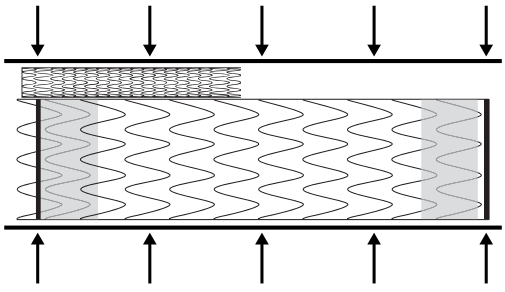

Figure 3: Schematic of representative TAG-Viabahn single chimney TEVAR subjected to uniform radial load. Illustrated is the apparent side view of the MSI RX650 tester; only two of the radial loading plates shown.

For BE ch-TEVAR, main endografts were first radially loaded to a diameter equivalent to 60% main endograft oversizing and maintained at the crimped diameter. Subsequently, a balloon-catheter mounted BE stent was positioned and deployed between the crimped main endograft and test aperture. Chimney grafts were positioned 1-2mm proximal to the main endograft covering, and aligned to lie between proximal main endograft stent struts where possible. Following BE stent deployment, the parallel devices were unloaded

from the crimped configuration. Due to test system availability, double BE ch-TEVAR combinations could not be considered in this study.

As only the unloading profiles of BE ch-TEVAR combinations capture parallel endograft behaviour, only unloading profiles and corresponding COF values are reported herein for each configuration. Values are normalized by measured main endograft length.

2.4. Mechanical deformation of parallel endografts

Mechanical deformations were evaluated via image analysis of video data acquired during the load-unload cycles. Briefly, a video recorder (Nikon D7100, Minato, Tokyo, Japan) was positioned in line with the test system, as shown in Figure 2. A purpose-built Matlab code (vR2016b, The MathWorks Inc., Natick, MA, USA) was developed to effectively sync both radial force and video data, and output corresponding video frames (images) at specified compression levels (diameters) of interest. Select video frames were then analysed using the open-source ImageJ2 image analysis software package (Fiji distribution) [15, 16].

Three measures, as originally described by Mestres et al. [17, 18], were used to quantify clinically-relevant endograft deformations. Specifically, gutter area, chimney graft compression, and graft infolding were assessed. In addition, main endograft compression was also evaluated. These metrics are defined below.

Gutter area was calculated as the total area of gaps forming between the main endograft, chimney graft, and test aperture boundaries, assessed as a percentage of equivalent lumen area. A lower gutter area represents reduced risk of adverse clinical events (i.e. type 1a endoleak).

Chimney graft compression was calculated as the relative decrease of visible chimney graft lumen area to the nominal labelled lumen area: CG compression = (1 - Measured/Nominal) x 100%. This metric is analogous to lumenal reduction as described by Demanget et al. [19]. Higher percentage values reflect increased device compression (i.e. loss of lumen area), and represent potential increased risk of adverse clinical events (e.g. loss of chimney graft patency).

Graft infolding was calculated as the maximal inward deflection of the main endograft covering into the lumenal area (in areas other than the chimney graft location), assessed as a percentage of lumen radius. Reduced graft infolding may represent reduced risk of potential adverse clinical events (e.g. thromboembolic events resulting from flow disturbances).

Main endograft compression was calculated as the relative decrease of visible main graft lumen area to the "ideal" ch-TEVAR main graft lumen area (i.e. the ideal MG outcome, conforming to both the vessel wall and CG). Lower values (i.e. less lumen reduction) represent better conformability.

All measurements were performed manually and were taken at the proximal edge of the corresponding graft covering at a single "ideal" aortic diameter (i.e. one level of oversizing). The ideal aortic diameter for each combination and the associated main endograft oversizing are given in Table 2. Details specifying the numerically determined ideal aortic diameter are provided in *Supplementary Material 1*. Video data of all experiments are provided in *Supplementary Material 2*. Measurement repeatability and the influence of so-called CG post-dilation are described in *Supplementary Material 3*.

Table 2: ch-TEVAR combinations and associated "ideal" aortic diameter and MG oversizing.

Combination	"Ideal" Aortic Diameter (mm)	MG Oversizing (%)
TAG-Viabahn	25.2	35
TAG-BeGraft	25.7	32
Valiant-Viabahn	30.4	32
Valiant-BeGraft	30.9	29
TAG-Viabahn (2x)	26.8	27
Valiant-Viabahn (2x)	31.6	26

3. Results

3.1. Device characterisation

The radial deformation-load profiles of TAG and Valiant main endografts are given in Figures 4a and 4b, respectively. COF and RRF values at both minimum and maximum instruction for use (IFU) recommended diameters, and for a range of oversizing, are given in Table 3. Characteristically, both radial load profiles exhibit biased stiffness as associated with Nitinol devices, albeit with differing intensity. Considering the indicated sizing for each device, the TAG exerts a COF between 0.15-0.55 N/mm, while the Valiant exerts a COF between 0.17-0.19 N/mm.

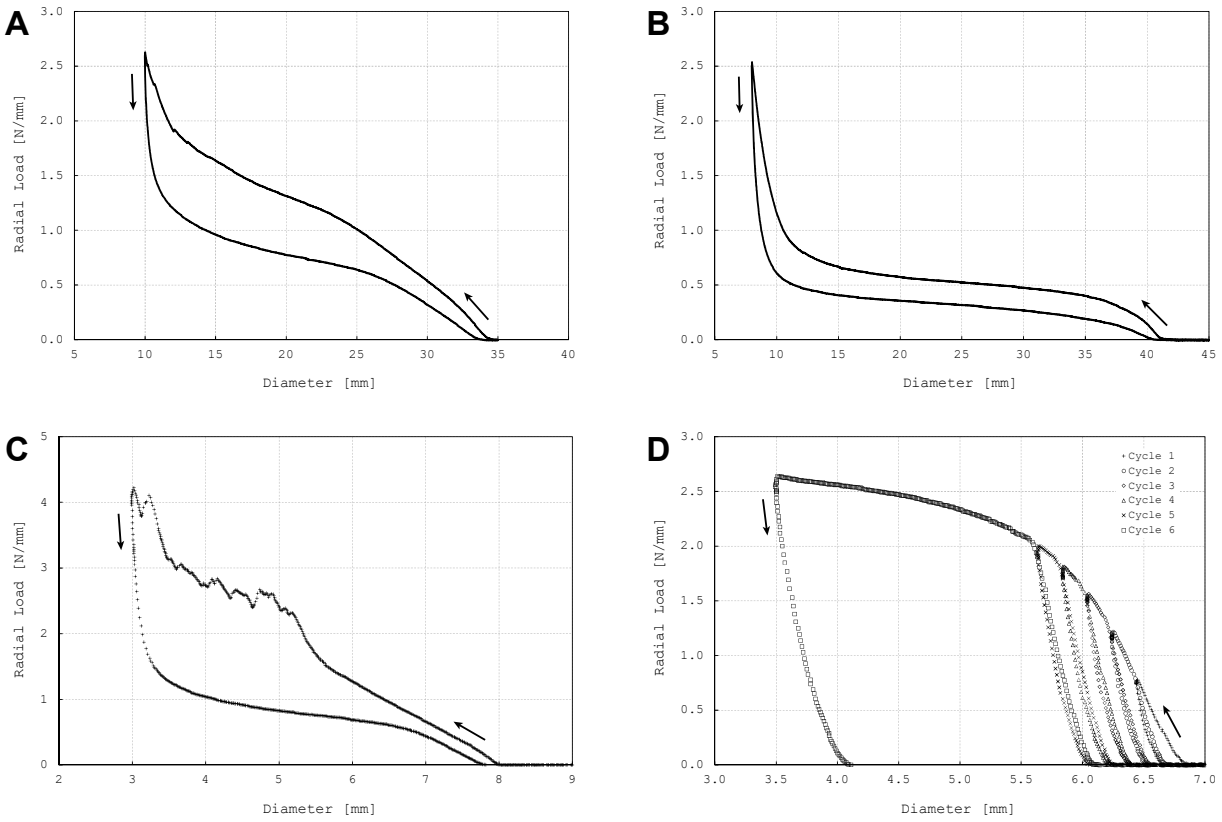

Figure 4: Device characterisation. Radial deformation-load profiles of (A) Gore TAG, (B) Medtronic Valiant, (C) Gore Viabahn, and (D) Bentley BeGraft endografts. Arrows denote loading-unloading directionality. In the case of self-expandable devices, loading corresponds to radial resistive force (RRF) and unloading corresponds to chronic outward force (COF).

The radial deformation-load profiles of the Viabahn and BeGraft chimney grafts are given in Figures 4c and 4d, respectively. Radial load measures appropriate to SE and BE devices are also reported in Table 3. Again, the SE Viabahn device exhibits biased stiffness. It was observed that the COF of the Viabahn device between the minimum and maximum IFU sizing range (0.15-0.58 N/mm) is comparable to the TAG main endograft device. The BE BeGraft device exhibits typical elastoplastic behaviour. Importantly, it was observed via the stepped multi-cycle test that the last unloading line is approximately parallel to all other unloading lines and to all reloading lines. When compressed to a diameter equivalent to the maximum oversizing diameter of its SE counterpart (6.6mmOD), the BeGraft's radial strength was found to be 0.76 N/mm.

Table 3: Endograft COF, RRF, and RS characterisation. All values reported as N/mm.

Oversizing	TAG		Valiant		Viabahn		BeGraft
	COF	RRF	COF	RRF	COF	RRF	RS*
Min. OS (IFU)	0.15	0.32	0.17	0.37	0.16	0.36	0.76
Max. OS (IFU)	0.55	0.83	0.19	0.40	0.58	0.90	
10% OS	0.25	0.45	0.16	0.36	–	–	
20% OS	0.45	0.70	0.22	0.43	–	–	
30% OS	0.59	0.91	0.26	0.46	–	–	
40% OS	0.66	1.07	0.28	0.49	–	–	
50% OS	0.71	1.18	0.30	0.51	–	–	
60% OS	0.75	1.25	0.32	0.52	–	–	

COF = chronic outward force; *RRF* = radial resistive force; *RS* = radial strength; *OS* = oversizing; *IFU* = instructions for use
*RS reported for unloading line-load profile intercept at 6.6mmOD

3.2. Radial loading profiles of ch-TEVAR

Radial deformation-load profiles of the single ch-TEVAR combinations are given in Figures 5a (TAG-Viabahn/BeGraft) and 5b (Valiant-Viabahn/BeGraft), and of the double ch-TEVAR combinations are given in Figures 5c (TAG-Viabahn) and 5d (Valiant-Viabahn). COF values for a range of main endograft oversizing, including the "ideal" aortic diameter, are reported in Table 4.

An increase in COF was observed for all ch-TEVAR combinations. This upward shift is exacerbated at increased levels of main endograft oversizing, such as those typically encountered during ch-TEVAR. In the case of TAG ch-TEVAR, the SE configuration exhibited 5.1x COF (from 0.15 to 0.77 N/mm) while the BE configuration exhibited 4.6x COF (from 0.15 to 0.69 N/mm) compared to standard TEVAR at minimum IFU oversizing. Considering Valiant ch-TEVAR, the SE configuration exhibited 1.9x COF (from 0.17 to 0.33 N/mm) while the BE configuration exhibited 1.8x COF (from 0.17 to 0.31 N/mm) compared to baseline.

Similar to the single chimney cases, an increase in COF was observed for both double chimney combinations. Again, this upward shift is exacerbated at increased levels of main endograft oversizing. In the case of TAG double chimney TEVAR, 4.5x COF was measured (from 0.15 to 0.68 N/mm). Considering Valiant double chimney TEVAR, 1.8x COF was measured (from 0.17 to 0.31 N/mm). Notably, no appreciable difference in COF values was observed between single and double chimney cases (e.g. 0.77 vs. 0.68 N/mm and 0.33 vs. 0.31 N/mm for TAG-Viabahn and Valiant-Viabahn cases, respectively), with the decrease in COF associated with the reduced level of main endograft oversizing required to achieve the ideal aortic diameter in the double chimney configuration.

3.3. Deformation behaviour of parallel endografts

All single chimney combinations exhibited gutters, both chimney and main endograft compression, as well as graft infolding. Endograft deformations resulting from radial (un)loading to an "ideal" ch-TEVAR vessel diameter are shown in Figure 6. Measured deformation values are reported in Table 5. The absolute largest total gutter area was determined to be 52.5mm^2, or 7.0% of lumen area, and was associated with the Valiant-BeGraft combination. Conversely, smaller gutter areas were associated with the SE chimney grafts, with the TAG-Viabahn combination resulting in the lowest measured gutter area equivalent to 3.2mm^2, or 0.6% of lumen area.

Chimney graft compression was most evident in configurations with Viabahn devices. The highest degree of compression was associated with the TAG-Viabahn combination, with a 67% chimney lumen cross-section

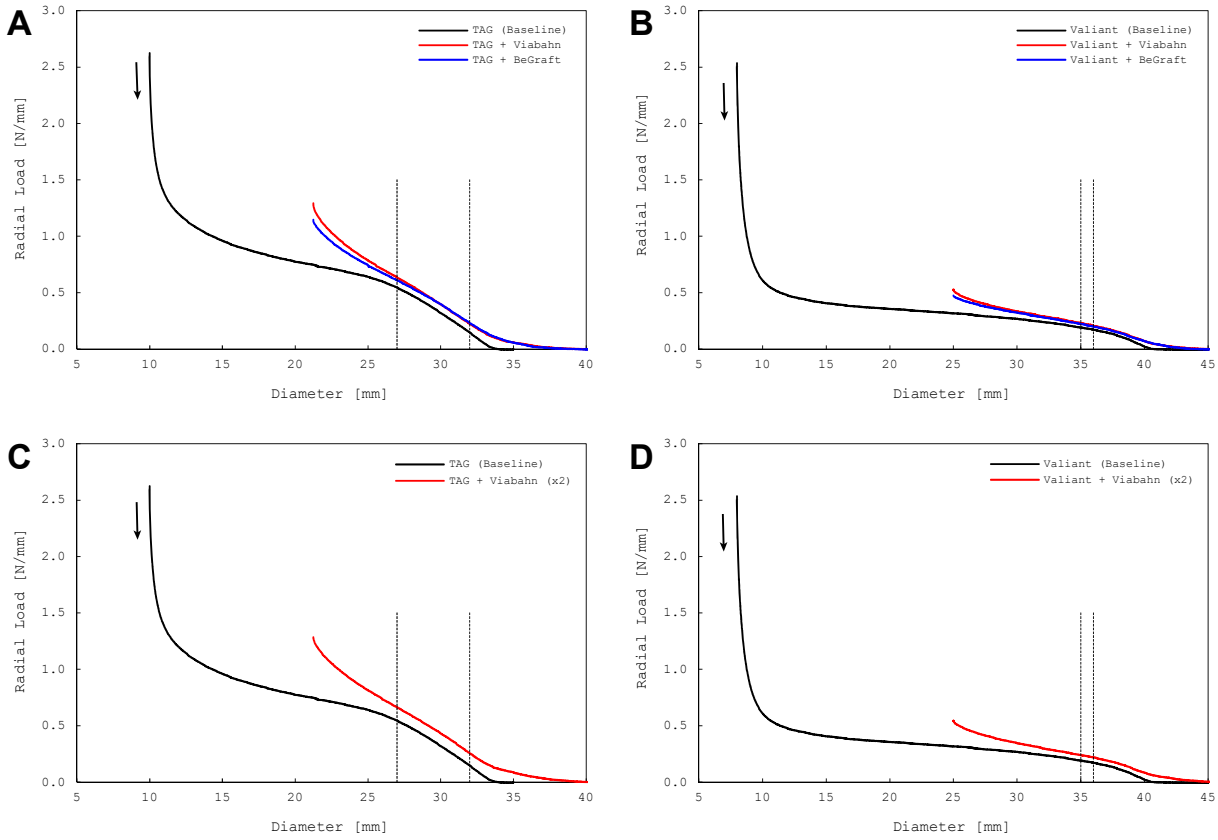

Figure 5: Radial deformation-load profiles of ch-TEVAR. (A) Single chimney TAG-Viabahn and TAG-BeGraft, (B) single chimney Valiant-Viabahn and Valiant-BeGraft, (C) double chimney TAG-Viabahn, and (D) double chimney Valiant-Viabahn. Arrows denote unloading directionality and correspond to chronic outward force (COF). Unloading curves obtained from MG characterisation are included to provide a baseline measure. Vertical lines indicate manufacturer IFU oversizing range.

Table 4: Chronic outward force of ch-TEVAR at the "ideal" aortic diameter and for a range of oversizing.

Oversizing	Chronic Outward Force (N/mm)					
	TAG-Viabahn	TAG-BeGraft	Valiant-Viabahn	Valiant-BeGraft	TAG-Viabahn (2x)	Valiant-Viabahn (2x)
"Ideal" OS	0.77	0.69	0.33	0.31	0.68	0.31
Min. OS (IFU)	0.22	0.23	0.21	0.20	0.26	0.22
Max. OS (IFU)	0.63	0.61	0.23	0.22	0.66	0.24
10% OS	0.32	0.32	0.20	0.19	0.36	0.21
20% OS	0.53	0.52	0.27	0.26	0.56	0.27
30% OS	0.70	0.67	0.32	0.31	0.73	0.33
40% OS	0.85	0.80	0.37	0.35	0.87	0.38
50% OS	1.01	0.93	0.42	0.40	1.03	0.44
60% OS	1.29	1.15	0.53	0.47	1.28	0.54

"Ideal" aortic diameter determined as per Supplementary Material 1;
OS – oversizing; *IFU* – manufacturer instructions for use

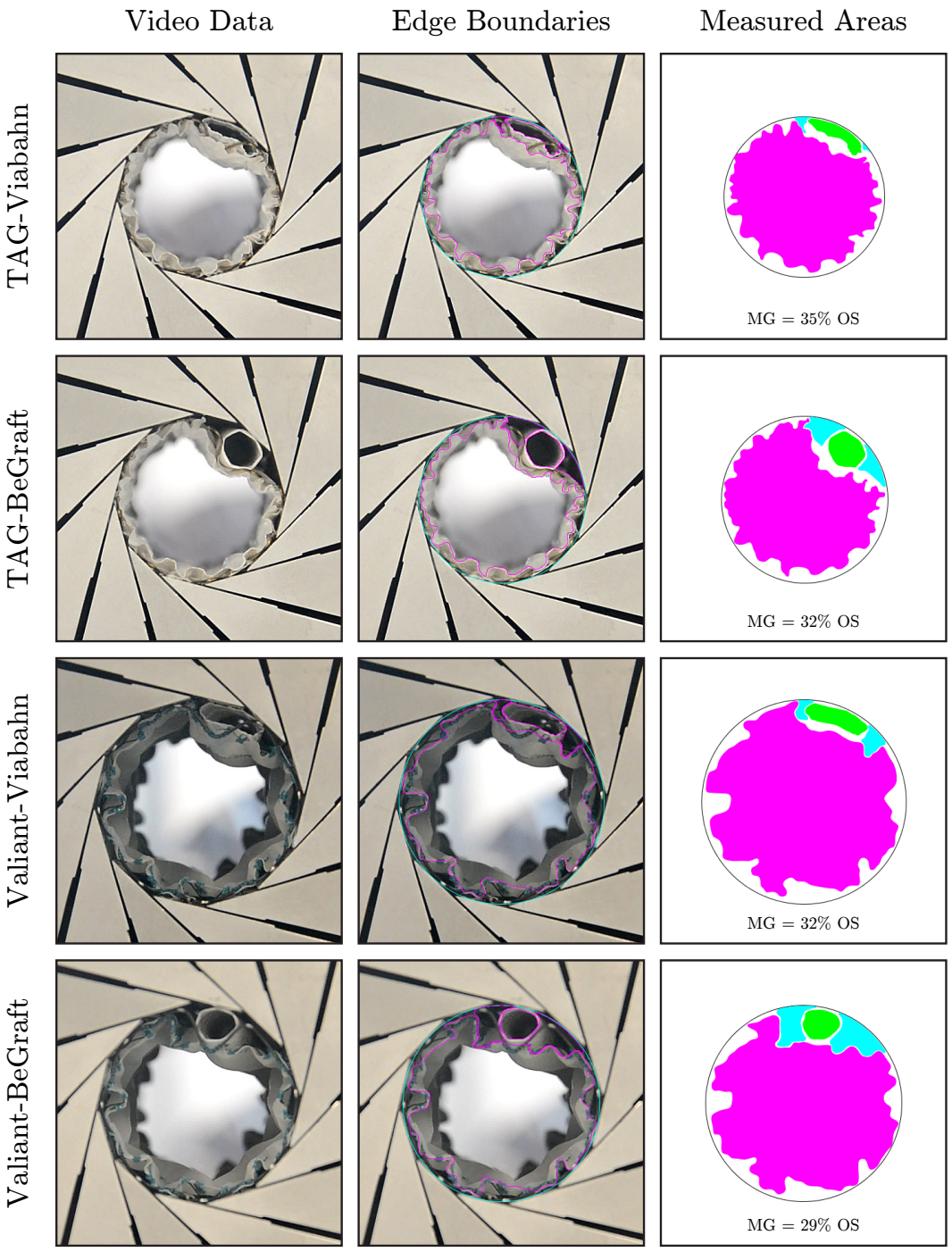

Figure 6: Deformations of single chimney parallel endografts. (Left) Synced video frame at the ideal aortic diameter; (center) constructed edge boundaries of MSI RX650 inscribed diameter, graft lumens, and gutter boundaries; (right) measured gutter (*cyan*), main endograft (*magenta*), and chimney graft (*green*) areas. Equivalent main endograft oversizing reported with respect to ideal aortic diameter.

Table 5: Deformation measures of parallel endografts in a single chimney configuration at the ideal aortic diameter for the MG-CG combination. Data reported as raw values (normalized).

	Gutter Area (mm^2)	Chimney Graft Area (mm^2)	Main Graft Area (mm^2)	Max. Graft Infolding (mm)
TAG-Viabahn	3.2 (0.6%)	16.7 (67%)	378.3 (15%)	3.2 (26%)
TAG-BeGraft	24.3 (4.7%)	23.6 (39%)	366.4 (24%)	2.8 (22%)
Valiant-Viabahn	13.4 (1.9%)	21.9 (56%)	556.6 (17%)	4.2 (28%)
Valiant-BeGraft	52.5 (7.0%)	21.7 (44%)	558.7 (21%)	4.1 (26%)

Normalizations: Lower is better across all metrics

reduction. Both BeGraft combinations exhibited lower compression in ch-TEVAR, with lumenal reductions of 39% and 44% for the TAG and Valiant configurations, respectively.

Regarding main endograft deformation behaviour, parallel configurations containing Viabahn chimneys exhibited lower lumen reduction, and thus higher levels of conformability, compared to BeGraft configurations. Between chimney graft pairs, conformability was measured to be 15% and 17% for TAG/Valiant-Viabahn and 24% and 21% for TAG/Valiant-BeGraft. When considering graft infolding, Valiant combinations exhibited the highest absolute measures (4.1mm and 4.2mm for BeGraft and Viabahn combinations, respectively). When normalized to lumen radius, infolding ranged from 22-28% across all combinations.

Gutters, graft compression, and graft infolding were also observed in the double chimney configurations considered in this study. Parallel endograft deformations resulting from radial (un)loading to an "ideal" aortic diameter are shown in Figure 7. Measured deformation values are reported in Table 6.

Table 6: Deformation measures of parallel endografts in a double chimney (Viabahn 2x) configuration at the ideal aortic diameter for the MG-CG combination. Data reported as raw values (normalized).

	Gutter Area (mm^2)	CG_1 Area (mm^2)	CG_2 Area (mm^2)	MG Area (mm^2)	Max. Infolding (mm)
TAG	9.4 (1.7%)	35.9 (29%)	35.2 (30%)	369.2 (18%)	3.2 (24%)
Valiant	15.0 (1.9%)	32.7 (35%)	27.1 (46%)	578.6 (14%)	4.0 (25%)

Normalizations: Lower is better across all metrics;
CG_1: left hand side Viabahn; CG_2: right hand side Viabahn

In both cases, four gutters were identified, and similar total gutter areas measured when normalized to lumenal area. However, total gutter area tripled in the double chimney TAG-Viabahn case compared to its single chimney counterpart (0.6% vs. 1.7% of lumen area), whereas gutter area remained constant in the case of double chimney Valiant-Viabahn compared to its single chimney counterpart (1.9% lumen area in both cases). Notably, chimney graft compression was lessened in the case of TAG-Viabahn double chimney TEVAR (29% and 30%, versus 67% in the single chimney case). A similar observation was made in the case of the Valiant-Viabahn, although to a lesser extent (35% and 46%, versus 56% in the single chimney case).

Regarding main endograft deformation, the TAG-Viabahn and Valiant-Viabahn double chimney combinations exhibited 18% and 14% conformability, respectively. The degree of double chimney graft infolding normalized to lumen radius was measured to be 24% and 25% in the Valiant and TAG cases, respectively.

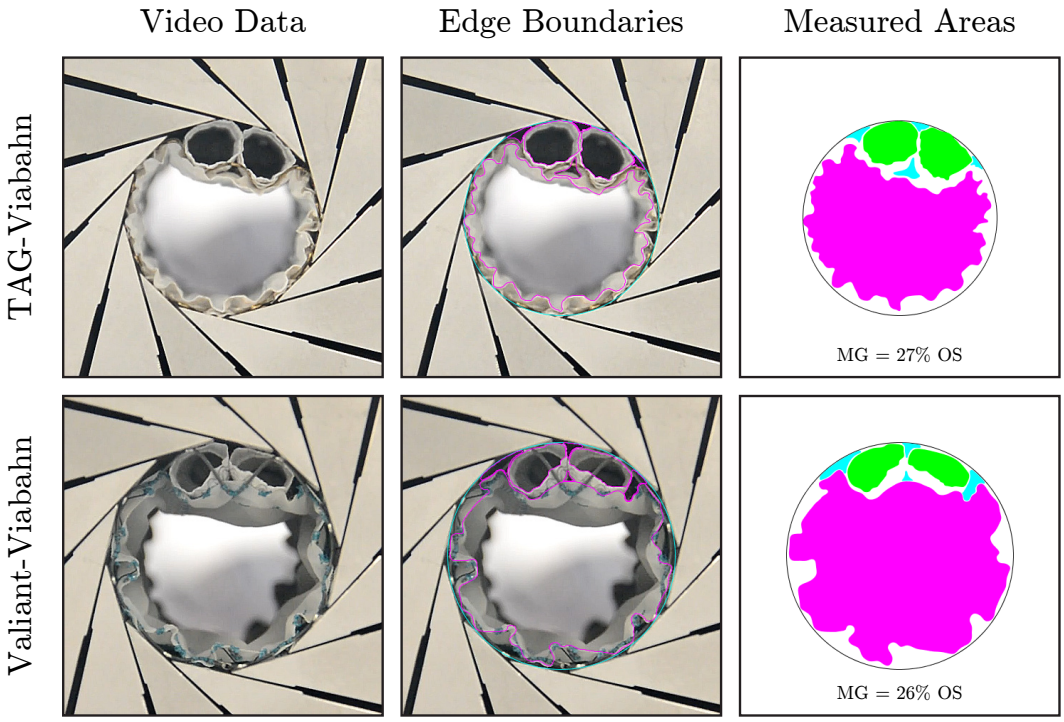

Figure 7: Deformations of double chimney parallel endografts. (Left) Synced video frame at the ideal aortic diameter; (center) constructed edge boundaries of MSI RX650 inscribed diameter, graft lumens, and gutter boundaries; (right) measured gutter (*cyan*), main endograft (*magenta*), and chimney graft (green) areas. Equivalent main endograft oversizing reported with respect to ideal aortic diameter.

4. Discussion

4.1. Device characterisation

Four commercially available endografts have been characterised according to their mechanical response to uniform radial load. The main endografts investigated represent two distinct stent-graft types: a continuous helical undulating wire frame design with a partially uncovered proximal stent (Gore TAG), and a discrete multiple stent-ring design with a flared proximal bare stent (Medtronic Valiant). Likewise, the chimneys represent two distinct chimney graft types: a SE helical undulating wire frame design (Gore Viabahn), and a BE open-cell frame design (Bentley BeGraft). As such, this work captures a number of relevant device combinations.

The results of the present study emphasize the significantly different radial load profiles, and hence device-artery interactions, of endografts used in clinical practice. Considering the main endografts and the associated COFs reported here, use of the TAG device can result in a threefold increase in radial load exerted onto an aortic wall if compared to a separate procedure employing a Valiant device. Notably, the main endografts investigated in this study exhibit considerably different behaviour at increasing levels of oversizing: the TAG demonstrates a generally constant increase in radial load values, whereas the Valiant tends towards a plateau over a similar range. In other words, the devices exhibit differing rates of radial load increase per radial compression (i.e. slope), with the COF of Valiant relatively insensitive to increases in oversizing. Clinically, this suggests that inadvertent/excessive oversizing is potentially less detrimental with Valiant compared to TAG.

The non-uniform loading profile of the Viabahn device past the recommended sizing level was attributed to the intricate structure of the Viabahn stent frame, whereby adjacent struts were believed to have come into contact and subsequently deflect to accommodate further diameter reduction. This behaviour occurred at radial compression levels in excess of 50% OS, and so deemed inconsequential to the *in vivo* scenario (where the maximum indicated oversizing is approximately 20%) or subsequent ch-TEVAR experiments as such excessive radial compression was not observed. Similarly, the sharp increase in radial load of both main endografts at excessively high levels of compression (i.e. those approaching constrained delivery diameter) was attributed to stent strut and graft self-contact.

In general, the behaviour reported here is consistent with trends described by De Bock et al. [20] and Morris et al. [21] for AAA devices; for example, "biased stiffness" during loading-unloading as well as distinct differences between endograft types. Recently, Matsumoto et al. [22] reported radial force measurements of three thoracic aortic endografts, including TAG and Valiant types. In that study, a different experimental technique was employed and radial deformation-load profiles were not reported, preventing direct comparisons. Nonetheless, the general observations of that study corroborate the findings here: TAG endografts exert higher radial loads onto the aortic wall compared to Valiant devices.

Regarding the chimney grafts investigated in this study, two different sizes (diameters) were intentionally selected. Specifically, the SE Viabahn was chosen to be one size larger than the BE BeGraft, as per clinical practice at our institution. The mechanical behaviour of peripheral stents has been reported in a select number of studies. However, those studies do not report response to uniform radial load [23–25], nor do they give detailed descriptions of the experimental/reporting methods used [22, 26], limiting their utility when evaluating ch-TEVAR.

The chimney graft characterisation presented here highlights the distinct and fundamental differences of endograft types and serves to clarify differing qualitative descriptions of parallel endograft behaviour found in the literature. Numerous studies have described the behaviour of chimneys based on their supposed "radial force" (see, for example, [9, 17, 18]), however, such ambiguous terminology confounds meaningful analysis of ch-TEVAR device combinations when comparing SE and BE chimney graft types. As made evident here, BE devices do not exert a radial force per se; their behaviour is strictly governed by their radial strength (i.e. ability to withstand deformation), whilst SE devices intrinsically have no radial strength limitation (i.e. they will elastically recover even after complete flattening/radial crushing) [27]. Thus, the more appropriate comparator is chimney graft radial stiffness: the resistance to diametric compression due to radial load. By simple consideration of the governing material behaviour of BE versus SE devices, a BE device will always have higher radial stiffness compared to a comparable SE device. The detailed device characterisation and

associated COF, RRF, and RS profiles reported in this study serve as the "on-label" baseline values to which the "off-label" ch-TEVAR configurations can be compared.

4.2. Benchtop ch-TEVAR

Recently, a series of *in vitro* studies have reported on the behaviour of parallel endografts used to treat challenging AAAs [17, 18, 28–32]. These studies, which provide compelling insights into the behaviour of devices during chimney type procedures, have solely focused on presenting geometrical data (and in the case of Boersen et al. [31], volumetric flow) and so were strictly limited to qualitative observations regarding device-device and device-artery interactions. The distinctly unique aspect of this investigation is the coupling of radial load profiles and corresponding mechanical deformations with the use of a radial force testing system and video (image) analysis. Given the device sizes available, the "ideal" aortic diameter for which a device combination would be selected in clinical practice was numerically determined based upon the method proposed by Kölbel [8]; with its intuitive geometric underpinnings and applicability to an *in vitro* context, this approach was deemed most suitable for this study. Dependent on device combination, the level of oversizing analysed here ranged from 26 - 35%, representing the upper OS range seen in clinical practice [33–36].

Mechanical deformation measures have been normalized in a manner similar to that described by Mestres et al. [17, 18]. Of note, the deformed main endograft area has also been reported here and has been normalized using the calculated "ideal" ch-TEVAR main endograft lumen area. Finally, as all previously reported *in vitro* chimney studies have relied on CT reconstructions where it is not possible to explicitly identify graft edge boundaries, this is the first study to provide quantitative data on the degree of graft infolding. Similarly, gutters and both chimney and main endograft lumen areas reported here are based on clearly defined graft edge boundaries.

4.3. Chronic outward force during ch-TEVAR

The results presented here demonstrate a marked increase in COF during both single and double ch-TEVAR, and for both SE and BE chimney graft types, compared to that anticipated in standard TEVAR. Dependent on configuration, ch-TEVAR can result in a fivefold increase in COF. In general, rates of COF increase per radial compression (i.e. slope) were observed to follow baseline measures between the minimum and maximum IFU indicated levels of oversizing. The increase in COF over baseline was further exacerbated at increased levels of oversizing (i.e. in the "off-label" scenario), as would typically be encountered in ch-TEVAR. Moreover, COF was consistently higher for TAG compared to Valiant across all combinations, with more than a twofold difference at the "ideal" aortic diameter. Although there exists no clearly defined "safe" COF threshold, apart from the implied manufacturer specified maximum oversizing, a systematic review by Canaud et al. [37] demonstrated that increased endograft oversizing (and hence COF) translated to an increased risk of aortic wall damage (as manifested by retrograde type A aortic dissection). The COFs reported here highlight the device dependent variability in potential aortic wall loading during ch-TEVAR procedures. Indeed, clinicians may need to exercise more caution with TAG oversizing in the presence of chimney grafts as COFs are up to 3x as affected by oversizing compared to Valiant.

There was found to be a minimal difference in COF between SE and BE ch-TEVAR. This finding is of particular interest given that BE endografts do not possess a radial force per se, whilst SE devices inherently do. The quasi-static nature of the experimental setup necessitates that force interactions between devices and the test aperture (analogous to a rigid vessel wall) must be balanced. Inspection of Figure 6 reveals that SE chimney grafts are prone to deformation. This deformation leads to a more uniformly distributed chimney graft contact against the apparent aortic wall. In contrast, the BE device retains its circular shape, limiting total contact area. Therefore, it follows that BE type chimney grafts may result in COF localizations onto the adjacent aortic segment, potentially leading to aortic wall stress concentrations.

4.4. Mechanical deformations during ch-TEVAR

This study illustrates that endograft deformations during ch-TEVAR are dependent on device type. Combinations employing BE chimney grafts exhibit larger gutter areas whilst maintaining their circular

cross-sections. Conversely, combinations employing SE chimney grafts presented with comparatively lower gutter areas, however, increased rates of lumen compression. Such behaviour is attributed to the difference in radial stiffness between chimney types. The direct comparison of results presented here to those reported by other groups is not wholly appropriate due to the differences in main endografts studied (TAA vs. AAA), experimental setup (RX650 tester vs. silicone models), and imaging techniques used (video vs. CT analysis). Nevertheless, these trends are similar to those of *in vitro* ch-EVAR and further corroborate the notion that SE compression leads to reduced gutter areas by deforming into the free (gutter) space [17, 18].

Notably, this is the first study to present detailed depictions of endograft inflow areas, as the methods employed here allow for exact delineation of the endograft boundary. The distinct variability in inflow shape between device types is attributed to the differences in stent design (for both main and chimney grafts) as well as graft attachment mechanisms (for main grafts). Interestingly, in the case of Valiant configurations it was observed that the fine Nitinol support wire at the proximal edge of the graft covering deflected into the lumenal area. Moreover, in the case of the BeGraft combination, this deflection contributed towards an increase in gutter area. However, the difference in stent design/graft attachment mechanism did not influence maximal endograft infolding; although the Valiant device presented with the highest absolute degree of infolding, when normalized to lumen radius, both main graft types exhibited nearly equivalent measures.

Finally, this is the first study to report deformation data on multiple parallel endografts arranged in an adjacent fashion as would be anticipated in some cases of double ch-TEVAR. The salient observations here pertain to chimney compression: in the case of double ch-TEVAR, adjacent chimney grafts appear to radially reinforce each other, limiting the degree of chimney compression. This reinforcement effect, however, was somewhat mitigated in the Valiant configuration due to chimney graft interactions with the proximal bare stent. These observations, when coupled with the behaviour of lumen deformations in the single chimney case, provide compelling insights into the potential best *in vivo* arrangement of endografts during double chimney TEVAR.

5. Limitations

Considering the benchtop nature of the work presented in this investigation, results should be viewed within the experimental context described herein and its associated limitations. First, the inherent elasticity of the aorta is not accounted for in this study, due to the necessary rigid nature of the test system. Similarly, experiments have been run in displacement control in a seemingly continuous loading-unloading fashion. Although endograft deformations have been evaluated in an essentially quasi-static manner, oversizing has been achieved by loading each endograft from an unconstrained state, and subsequently unloading to the analysis diameter. Accordingly, the apparent endograft deformations are dependent on the previous time instance, which is not the case in the clinical scenario.

Secondly, the test setup does not account for aortic pressure, nor pulsatile blood flow. It is anticipated that internal pressures and flow acting on the endograft covering would likely influence its configuration, and thus the associated measures reported in this study.

Finally, a limited number of devices were investigated, restricting quantitative findings to the specific devices and configurations described. Specifically, the main endografts used in this investigation (which were limited in availability to our group) cannot provide a like-for-like comparison given their differing nominal diameters. Nevertheless, the observations reported here do allow for meaningful comparisons across a wide anatomical range. Similarly, devices were reused with the potential of accumulated plasticity between loading cycles. Of note, the Gore TAG comes constrained in an ePTFE sleeve which remains implanted upon device deployment. For the sake of simplicity, and to isolate the effects of the endoprosthesis alone, this sleeve was removed. Likewise, owing to the experimental setup, it was only possible to deploy the BE devices in an orientation such that its distal end was subject to evaluation. Chimney grafts were also assumed to have "landed" parallel to each main graft, while they may in fact take oblique routes *in vivo*. It is also recognized that the endografts used in this study are previous generation devices, with some next-generation devices already in clinical use.

6. Conclusions

In this study, four single chimney and two double chimney TEVAR configurations have been evaluated when subjected to uniform radial load. Chimney TEVAR results in increased aortic wall loading when compared to standard TEVAR. For the devices considered here, the magnitude of radial load acting on the aortic wall is dependent on main endograft type. Mechanical deformations of parallel endografts during ch-TEVAR were found to be dependent on chimney graft type, and in the case of double ch-TEVAR, deployed arrangement. Additional investigation is warranted to better identify best device combinations and configurations during ch-TEVAR.

Conflict of interest

The authors declare no potential conflicts of interest with respect to the research, authorship, and/or publication of this article.

Funding

None.

Acknowledgements

The authors would like to thank Hannes Feldman of Admedes GmbH for technical support during radial force testing. BeGraft samples were generously provided by Bentley Innomed GmbH.

References

[1] Sincos IR, da Silva ES, Belczak SQ, et al. Histologic analysis of stent graft oversizing in the thoracic aorta. *Journal of Vascular Surgery*, 58(6):1644–1651, 2013.

[2] Alberta HB, Secor JL, Smits TC, et al. Comparison of thoracic aortic diameter changes after endograft placement in patients with traumatic and aneurysmal disease. *Journal of Vascular Surgery*, 59(5):1241–1246, 2014.

[3] Criado FJ. Parallel stent graft techniques to facilitate endovascular repair in the aortic arch. In *Endovascular Aortic Repair – Current Techniques with Fenestrated, Branched and Parallel Stent-Grafts*, pages 543–554. Springer, 2017.

[4] Ahmad W, Mylonas S, Majd P, and Brunkwall JS. A current systematic evaluation and meta-analysis of chimney graft technology in aortic arch diseases. *Journal of Vascular Surgery*, 66(5):1602–1610.e2, 2017.

[5] Czerny M, Schmidli J, Adler S, et al. Current options and recommendations for the treatment of thoracic aortic pathologies involving the aortic arch: An expert consensus document of the European Association for Cardio-Thoracic Surgery (EACTS) & the European Society for Vascular Surgery (ESVS). *European Journal of Vascular and Endovascular Surgery*, 57(2):165–198, 2019.

[6] Lachat M. *Multiple chimneys: Techniques, results and limitations.* Presented at the 33rd CX Symposium. London, UK, 2011.

[7] Chou HW, Chan CY, Wang SS, and Wu IH. How to size the main aortic endograft in a chimney procedure. *The Journal of Thoracic and Cardiovascular Surgery*, 147(3):1099–1101, 2014.

[8] Kölbel T, Carpenter SW, Taraz A, et al. How to calculate the main aortic graft-diameter for a chimney-graft. *The Journal of Cardiovascular Surgery*, 57(1):66–71, 2016.

[9] Fazzini S, Ronchey S, Orrico M, et al. Over-SIRIX: A new method for sizing aortic endografts in combination with the chimney grafts – early experience with aortic arch disease. *Annals of Vascular Surgery*, 46(Supplement C):285–298, 2018.

[10] ASTM International. *ASTM F3067-14: Guide for Radial Loading of Balloon Expandable and Self Expanding Vascular Stents.* West Conshohocken, PA, USA, 2014.

[11] Cabrera MS, Oomens CWJ, and Baaijens FPT. Understanding the requirements of self-expandable stents for heart valve replacement: Radial force, hoop force and equilibrium. *Journal of the Mechanical Behavior of Biomedical Materials*, 68: 252–264, 2017.

[12] Egron S, Fujita B, Gullón L, et al. Radial force: An underestimated parameter in oversizing transcatheter aortic valve replacement prostheses: In vitro analysis with five commercialized valves. *ASAIO Journal*, 64(4):536–543, 2018.

[13] Dabir D, Feisst A, Thomas D, et al. Physical properties of venous stents: An experimental comparison. *CardioVascular and Interventional Radiology*, 41(6):942–950, 2018.

[14] Duerig TW, Tolomeo DE, and Wholey M. An overview of superelastic stent design. *Minimally Invasive Therapy & Allied Technologies*, 9(3-4):235–246, 2000.

[15] Schindelin J, Arganda-Carreras I, Frise E, et al. Fiji: an open-source platform for biological-image analysis. *Nature Methods*, 9(7):676–682, 2012.

[16] Rueden CT, Schindelin J, Hiner MC, et al. ImageJ2: ImageJ for the next generation of scientific image data. *BMC Bioinformatics*, 18(1):529, 2017.
[17] Mestres G, Uribe JP, Garca-Madrid C, et al. The best conditions for parallel stenting during EVAR: An in vitro study. *European Journal of Vascular and Endovascular Surgery*, 44(5):468–473, 2012.
[18] Mestres G, Yugueros X, Apodaka A, et al. The best in vitro conditions for two and three parallel stenting during endovascular aneurysm repair. *Journal of Vascular Surgery*, 66(4):1227–1235, 2017.
[19] Demanget N, Avril S, Badel P, et al. Computational comparison of the bending behavior of aortic stent-grafts. *Journal of the Mechanical Behavior of Biomedical Materials*, 5(1):272–282, 2012.
[20] De Bock S, Iannaccone F, De Beule M, et al. Filling the void: A coalescent numerical and experimental technique to determine aortic stent graft mechanics. *Journal of Biomechanics*, 46(14):2477–82, 2013.
[21] Morris L, Stefanov F, Hynes N, Diethrich EB, and Sultan S. An experimental evaluation of device/arterial wall compliance mismatch for four stent-graft devices and a multi-layer flow modulator device for the treatment of abdominal aortic aneurysms. *European Journal of Vascular and Endovascular Surgery*, 51(1):44–55, 2016.
[22] Matsumoto T, Matsubara Y, Aoyagi Y, et al. Radial force measurement of endovascular stents: Influence of stent design and diameter. *Vascular*, 24(2):171–176, 2016.
[23] W.L. Gore & Associates, Inc. *Mechanical Properties of Nitinol Stents and Stent-grafts: Comparison of 6mm Diameter Devices*, 2011.
[24] Teßarek J. *BeGraft peripheral: Stent design and technical aspects.* Presented at the Leipzig Interventional Course. Leipzig, Germany, 2016.
[25] Maleckis K, Deegan P, Poulson W, et al. Comparison of femoropopliteal artery stents under axial and radial compression, axial tension, bending, and torsion deformations. *Journal of the Mechanical Behavior of Biomedical Materials*, 75 (Supplement C):160–168, 2017.
[26] Verhoeven E and Katsargyris A. *First clinical experience with a new balloon-expandable stent graft: Potential advantages for side branch reconstruction during EVAR of complex pathologies.* Presented at the Leipzig Interventional Course. Leipzig, Germany, 2018.
[27] Duerig T and Wholey M. A comparison of balloon- and self-expanding stents. *Minimally Invasive Therapy & Allied Technologies*, 11(4):173–178, 2002.
[28] de Bruin JL, Yeung KK, Niepoth WW, et al. Geometric study of various chimney graft configurations in an in vitro juxtarenal aneurysm model. *Journal of Endovascular Therapy*, 20(2):184–190, 2013.
[29] Niepoth WW, de Bruin JL, Yeung KK, et al. A proof-of-concept in vitro study to determine if EndoAnchors can reduce gutter size in chimney graft configurations. *Journal of Endovascular Therapy*, 20(4):498–505, 2013.
[30] Niepoth WW, de Bruin JL, Lely RL, et al. In vitro feasibility of a sac-sealing endoprosthesis in a double chimney graft configuration for juxtarenal aneurysm. *Journal of Endovascular Therapy*, 21(4):529–537, 2014.
[31] Boersen JT, Donselaar EJ, Jebbink EG, et al. Benchtop quantification of gutter formation and compression of chimney stent grafts in relation to renal flow in chimney endovascular aneurysm repair and endovascular aneurysm sealing configurations. *Journal of Vascular Surgery*, 66(5):1565–1573, 2017.
[32] Overeem SP, Donselaar EJ, Boersen JT, et al. In vitro quantification of gutter formation and chimney graft compression in chimney EVAR stent-graft configurations using electrocardiography-gated computed tomography. *Journal of Endovascular Therapy*, 25(3):387–394, 2018.
[33] Shahverdyan R, Gawenda M, and Brunkwall J. Triple-barrel graft as a novel strategy to preserve supra-aortic branches in arch-tevar procedures: Clinical study and systematic review. *European Journal of Vascular and Endovascular Surgery*, 45(1):28–35, 2013.
[34] Mangialardi N, Serrao E, Kasemi H, et al. Chimney technique for aortic arch pathologies: an 11-year single-center experience. *Journal of Endovascular Therapy*, 21(2):312–323, 2014.
[35] Voskresensky I, Scali ST, Feezor RJ, et al. Outcomes of thoracic endovascular aortic repair using aortic arch chimney stents in high-risk patients. *Journal of Vascular Surgery*, 66(1):9–20, 2017.
[36] Shahverdyan R, Mylonas S, Gawenda M, and Brunkwall J. Single-center mid-term experience with chimney-graft technique for the preservation of flow to the supra-aortic branches. *Vascular*, 26(2):175–182, 2018.
[37] Canaud L, Ozdemir BA, Patterson BO, et al. Retrograde aortic dissection after thoracic endovascular aortic repair. *Annals of Surgery*, 260(2):389–395, 2014.